N91-24134

Reynolds Number Effects on the Transonic Aerodynamics of a Slender Wing-Body Configuration

S2-02
19849

James M. Luckring
NASA-Langley Research Center

Charles H. Fox, Jr.
NASA-Langley Research Center

Jeffrey S. Cundiff
George Washington University / USAF
Hampton, Virginia

Summary

Aerodynamic forces and moments for a slender wing-body configuration are summarized from an investigation in the Langley National Transonic Facility (NTF). The results include both longitudinal and lateral-directional aerodynamic properties as well as sideslip derivatives. Results have been selected to emphasize Reynolds number effects at transonic speeds although some lower speed results are also presented for context. The data indicate nominal Reynolds number effects on the longitudinal aerodynamic coefficients and more pronounced effects for the lateral-directional aerodynamic coefficients. The Reynolds number sensitivities for the lateral-directional aerodynamic coefficients were limited to high angles of attack.

Introduction

Recent interest has developed in advanced aerospace vehicles which are capable of very high speed flight. Examples of such vehicles include a variety of advanced transport concepts designed for supersonic cruise as well as transatmospheric vehicles such as the proposed X-30. These vehicles all tend to be slender due to high speed considerations, although they still embrace a wide range of configurational concepts (i.e., wing-bodies, waveriders, accelerators, etc.). The aerodynamic challenges for such vehicles are by no means limited to high speed concerns such as cruise design or aerothermal heating. Most aerodynamic subdisciplines (e.g., stability and control, propulsion integration, transonic flow, high angle of attack, etc.) present unique and often conflicting challenges for these vehicles. Extending the current aerodynamic data base for such a broad range of concepts and issues would constitute a vast research endeavor and possibly require more time than is practical. However, focused investigations for selected configurations could provide insight to certain fundamental aerodynamic issues in a timely manner.

The present investigation is directed toward transonic Reynolds number effects for a slender wing-body configuration of the accelerator class. Some discussion of lower speed and lower Reynolds number data is also provided for perspective. The accelerator class of configuration tends toward body-dominant conical geometries with slender wings. As a consequence, the wing and body related aerodynamics are very closely coupled. Some prominent aerodynamic features for this class of configuration include conical-like shock structures and boundary layer flows and, at high angles of attack, forebody separated flows along with wing (leading edge) vortex flows.

This research is part of a broader experimental program at NASA Langley. The purpose of this program is to (i) design a force-and-moment wind-tunnel model with suitable configuration parametrics which is based upon one of the configurational concepts and (ii) examine selected aerodynamic phenomena over an appreciable range of Reynolds numbers and Mach numbers. The status of this program will be briefly addressed.

PRECEDING PAGE BLANK NOT FILMED

Symbols

b	wing span
C_D	drag coefficient, Drag/ $q_\infty S_{ref}$
$C_{D,o}$	drag coefficient at zero lift
C_L	lift coefficient, Lift/ $q_\infty S_{ref}$
C_l	body-axis rolling-moment coefficient, Rolling Moment/ $q_\infty S_{ref} b$
C_{l_β}	beta derivative of body-axis rolling-moment coefficient
C_m	pitching-moment coefficient, Pitching Moment/ $q_\infty S_{ref} \bar{c}$
C_N	normal-force coefficient, Normal Force/ $q_\infty S_{ref}$
C_n	body-axis yawing-moment coefficient, Yawing Moment/ $q_\infty S_{ref} b$
C_{n_β}	beta derivative of body-axis yawing-moment coefficient
$\bar{c}$	mean aerodynamic chord of reference wing planform
ℓ	total body length
M_∞	freestream Mach number
q_∞	freestream dynamic pressure
R	Reynolds number based on ℓ
r_n	nose radius
S_{ref}	area of reference wing planform, extended to model centerline
α	angle of attack, degrees
β	angle of sideslip, degrees
θ_b	frustum angle, degrees
θ_c	cone angle, degrees
Λ	leading-edge sweep angle, degrees

Abbreviations

LTPT	Low Turbulence Pressure Tunnel
NTF	National Transonic Facility
UPWT	Unitary Plan Wind Tunnel

Configuration and Test Program

Basic geometric features of the configuration are presented in figure 1. The fuselage was comprised of a cone/cylinder/frustum with a cone half angle of 5 degrees, a boattail angle of 9 degrees, and an overall length of three feet. The maximum fuselage diameter was 12.87 percent of the body length and the sharp nose radius was approximately 0.014 percent of the body length. The delta wing was of unit aspect ratio (75.96 degrees leading-edge sweep) with a symmetric 4 percent thick diamond airfoil section and a span of 30 percent body length. The leading and trailing edges were sharp. The wing was mounted with zero incidence such that the trailing edge fell at 92 percent of the body length. Moments were referenced about the quarter chord point of the mean aerodynamic chord for the wing planform extended to the plane of symmetry; this occurred at 62 percent of the body length. The vertical tail had a leading-edge sweep of 70 degrees, a trailing-edge sweep of approximately -2 degrees, and a symmetric 4 percent thick diamond airfoil section. Additional details of the model geometry have been reported by Fox et al. (reference 1). A photograph of the model mounted in NTF is presented in figure 2.

The overall range of test conditions for the NTF experiment are summarized in figure 3. Reynolds numbers are based upon the reference body length of 3 feet. The tests were conducted for Mach numbers ranging from 0.3 to 1.15 and Reynolds numbers ranging from 18 million to 180 million. The maximum Reynolds number data were obtained at $M_\infty = 0.6$. Test conditions were accomplished with total pressures nominally ranging from 2.0 to 7.3 atmospheres and total temperatures nominally ranging from 120 down to -225 degrees Fahrenheit. The model was sting mounted on an internal six-component force balance. The support mechanism included a roll coupling so that pitch and roll could be combined to

achieve angle of attack and sideslip.

A more detailed description of the test program is presented in figure 4 along with the NTF tunnel envelope as reported by Fuller (reference 2). The test was structured such that (i) Reynolds number effects could be studied at a subsonic and a transonic freestream Mach number and (ii) Mach number effects could be studied at a low and a high Reynolds number. Both longitudinal and lateral-directional aerodynamic properties were investigated up to an angle of attack of approximately 20 degrees. Sideslip derivatives were computed from data taken at +4 and -4 degrees of sideslip. These data were only obtained at freestream conditions corresponding to the "corners" of the test matrix shown in figure 4. Results for the present paper are focused on the Reynolds number data taken at a freestream Mach number of 0.9.

The data were obtained in NTF with the test section floor and ceiling slotted and the side walls solid. The measurements have been compensated for temperature effects, and conventional corrections have been applied to the data for the effects of deflection due to load, flow angularity, and base pressure. These corrections were, in general, small. No buoyancy corrections have been applied to the data. However, these effects were also found to be small. Tests in NTF occurred in early February, 1988.

The test program for this wind-tunnel model encompasses additional facilities to NTF as shown in figure 5. In particular, the model design permits supersonic testing in the Langley Unitary Plan Wind Tunnel (UPWT) as well as low-speed Reynolds-number testing in the Langley Low Turbulence Pressure Tunnel (LTPT). Included in figure 5 is the tunnel envelope for UPWT as reported by Jackson et al. (reference 3), the tunnel envelope for LTPT as reported by McGhee et al. (reference 4), and an indication of the freestream conditions at which testing has been completed. Thus far, data have been obtained for Mach numbers ranging from 0.2 to 4.5 and Reynolds numbers ranging from 1 million to 180 million; these results have been obtained with the same wind-tunnel model. Preliminary supersonic results from the UPWT investigation may be found in the paper by Covell et al. (reference 5). Results from the LTPT experiment have been reported by Fox et al. (reference 1) as well as by Luckring et al. (reference 6).

Both the UPWT and the LTPT tests addressed a substantially broader range of configuration parametrics than was investigated in NTF. The configuration variables for the LTPT investigation included fuselage nose bluntness, vertical tails, and canards. The UPWT investigation included these same variables as well as wing incidence, longitudinal wing position, and wingtip-mounted vertical fins.

The current test program includes plans for further testing in the UPWT to obtain data at low supersonic speeds. In addition, a set of nominally half-scale models have been fabricated for testing at hypersonic speeds.

Results and Discussion

The general effects of Reynolds number on longitudinal aerodynamic properties are summarized in figure 6 for a freestream Mach number of 0.9. As would be expected, Reynolds number had minimal effects on the lift and pitching moment data. The lift-curve slope evidences a break at approximately 4 degrees angle of attack beyond which nonlinear lift effects are observed. The pitching moment data show a nose-down break at a comparable angle of attack. These effects are primarily associated with the separation-induced leading-edge vortex flow from the wing. The data of figure 6c show a reduction in the zero-lift drag coefficient of approximately 25 counts due to an increase in Reynolds number from 24 to 45 million. The shape of the drag polar was unaffected by this increase in Reynolds number. Further increases in Reynolds number had little effect on the drag.

The results of figure 6c include wave drag increments as indicated by the data presented in figure 7. Here the drag coefficient is presented for several freestream Mach numbers ranging from 0.6 to 1.15 at a fixed Reynolds number of 90 million. At a freestream Mach number of 0.9, the zero-lift drag coefficient has roughly doubled as compared to the results for a freestream Mach number of 0.6; this increment is primarily associated with wave drag. Additional discussion of the zero-lift drag rise will be included in the section regarding theoretical estimates. In general, the Reynolds number effects for the longitudinal forces and moments were nominal.

Contrary to the longitudinal results, Reynolds number has a more pronounced effect on the lateral-directional aerodynamic properties; this effect occurs at high angles of attack. An example is presented in figure 8 for the variation of yawing moment with angle of attack at zero sideslip. These data were obtained at a freestream Mach number of 0.3 over a range of Reynolds numbers in the LTPT investigation reported by Fox et al. (reference 1). All lateral-directional properties in this paper are presented in the body axis coordinate system.

The yawing moment is essentially zero up to a critical angle of attack of approximately 12 degrees. Beyond this angle of attack, nonzero values of the yawing moment develop due to asymmetric forebody separation and demonstrate a strong sensitivity to Reynolds number. However, the onset angle of attack for the asymmetric loads shows little effect of Reynolds number. The initial buildup of yawing moment (2 to 3 degrees beyond the onset angle) also shows little effect of Reynolds number. The critical angle of 12 degrees is on the order of twice the cone semiapex angle, as would be expected from previous forebody research such as has been reported by Keener and Chapman (reference 7). These yawing moment trends are representative of the other lateral-directional aerodynamic coefficients. These data, along with the other results reported by Fox et al. (reference 1), served as precursor information for the high Reynolds number investigation in NTF.

The model configuration for the data of figure 8 differs from the configuration for the NTF tests in two respects. First, the sharp nose used for the NTF experiments was a replacement for the one utilized for the LTPT test which had become damaged. The second difference is that the vertical tail was removed for the data presented in figure 8.

Reynolds number effects for the current investigation are first addressed by presenting results over a range of freestream Mach numbers at both a low and a high Reynolds number test condition, figure 9. Before addressing the Reynolds and Mach number effects, it should be noted that the yawing moment has the opposite sign at high angles of attack as compared to the results from the LTPT investigation (cf, figure 8). This indicates that the flow asymmetry has occurred in the opposite sense. This can be caused by either (i) minor differences in the geometry of the nose or (ii) minor differences in flow angularity between the tunnels. However, for each test the asymmetry tended to occur either with one sense or the other throughout the test; it was very repeatable.

At a Reynolds number of 24 million (figure 9a) the data show minimal Mach number effects for the angle-of-attack range investigated. A lack of sensitivity to Mach number was also observed by Fox et al. (reference 1) at a Reynolds number of 9 million for Mach numbers ranging from 0.2 to 0.375. However, at a Reynolds number of 90 million (figure 9b) the data do evidence compressibility effects for angles of attack in excess of approximately 16 degrees.

The results presented in figure 9 also demonstrate significant Reynolds number effects at high angles of attack. The nonlinear reversal in yawing moment which occurred at a Reynolds number of 24 million did not occur at a Reynolds number of 90 million within the angle of attack range investigated. The data presented in figure 10 indicate that this change in the high angle of attack yawing moment is generally associated with high Reynolds number flow. At a freestream Mach number of 0.6 (figure 10a) the data for the two lower Reynolds numbers both show the yawing moment reversal whereas the data for the two higher Reynolds numbers do not evidence this effect. The transonic case (figure 10b) shows a similar trend. In addition, the high Reynolds number yawing moments do not appreciably change beyond 16 degrees angle of attack. This effect was not observed at $M_\infty = 0.6$. It is difficult to determine from the data specific Reynolds numbers at which the changes occur.

The data of figure 10 show limited Reynolds number effects in the 10 to 16 degree angle of attack range. This differs from the results presented in figure 8 where Reynolds number sensitivities were manifested at only 2 to 3 degrees angle of attack beyond the onset angle of attack for flow asymmetry. Therefore, it appears that the angle of attack at which Reynolds number effects become evident in the lateral directional coefficients increases as the Reynolds number itself increases. Confirmation of this observation will require further testing.

Sideslip derivative data were obtained at nominally the limiting freestream conditions of the test matrix shown in figure 4. The results presented in figure 11 show compressibility effects on the lateral-directional stability derivatives at a low and a high Reynolds number. As was observed for the yawing moment data of figure 9, the low Reynolds number data (figure 11a) show virtually no compressibility

effect whereas at the high Reynolds number condition (figure 11b) significant compressibility effects are indicated for high angles of attack. The results presented in figure 12 indicate that Reynolds number effects were limited to high angles of attack and were most prevalent at low speeds. The data of figures 11 and 12 show that neither Mach number nor Reynolds number had any significant effects on the lateral-directional stability derivatives below approximately 14 degrees angle of attack.

Theoretical Estimates

A preliminary theoretical analysis of the longitudinal forces and moments was conducted to provide design loads as well as to provide some insight to the longitudinal aerodynamic phenomena. Calculations were performed with the vortex lattice program of Margason and Lamar (reference 8) as extended by Lamar and Gloss (reference 9) to account for separation-induced vortex lift effects by the leading-edge suction analogy of Polhamus (reference 10). This method was selected because it has proved over many years to provide reasonable estimates of longitudinal forces and moments for a wide range of applications as reported by Lamar and Luckring (reference 11), for example. The method was also chosen because (i) it tends to provide conservative load estimates (i.e., errors result in over predictions of the loads) and (ii) it is a very rapid method to utilize. These attributes are principally due to Polhamus' suction analogy concept which allows nonlinear integral properties associated with leading-edge vortex flows to be extracted from a simple linear theory computation.

Theoretical estimates for the effects of compressibility are presented in figure 13. The normal force results are for a fixed angle of attack of 10 degrees whereas the pitching moment results are for a fixed lift coefficient of 0.3. Differences between the attached flow theory and the vortex flow theory are due to the vortex lift increment predicted for the wing by the suction analogy. Although the trend with Mach number is reasonably well predicted by the theory, the magnitudes of normal force and pitching moment are not. The differences between the vortex-flow theory and the experiment are larger than would be expected from prior experience; they are primarily due to a poor representation of the fuselage in the computation as a flat plate. This approach neglects the nonlinear interaction of the leading-edge vortex with the thick body.

A surface grid representation of the configuration (without tail) is presented in figure 14 which illustrates the relative size of the body to the wing. Near the forward portion of the wing the body thickness will tend to crowd the leading-edge vortex off of the wing. This effect reduces the vortex lift increment which also results in a negative pitching moment increment for the assumed moment reference point. Methods which properly account for the vortex-body interaction have been shown to accurately predict force and moment properties for configurations similar to the one of the present investigation. An example has been given by Luckring and Thomas (reference 12) for the wing-body configuration tested by Stahl et al. (reference 13).

Computations for the zero-lift drag rise have also been performed using the analysis system reported by Middleton et al. (reference 14). Calculations are presented in figure 15 along with experimental results at a Reynolds number of 90 million. The theoretical drag is comprised of a skin friction increment based upon the method of Sommer and Short (reference 15) along with a standard supersonic wave drag increment; form drag effects were not included in these estimates.

The computed friction drag provides a reasonable estimate from which the transonic drag rise is evident. The experimental drag coefficient at a freestream Mach number of 0.3 is less accurate than the other data shown on the figure due to the reduced loads at this freestream condition. This relative difference in accuracy is conjectured to be a leading cause for the seemingly high experimental value of $C_{D,o}$ at this Mach number. The supersonic drag estimate is higher than the experimental value by approximately 60 counts. A comparable drag increment between theory and experiment was found by Compton (reference 16) for the boattail drag of a geometrically similar afterbody when suitably normalized.

Concluding Remarks

Selected results have been presented from an experimental investigation in the Langley National Transonic Facility (NTF) of a slender wing-body configuration. The tests were conducted at Reynolds numbers ranging from 18 million to 180 million based on total model length and at Mach numbers ranging from 0.3 to 1.15. The configuration is similar to the accelerator class of vehicles which have been considered (along with other configurational concepts) for future high-speed aerospace vehicles.

Experimental results for the effects of Mach number and Reynolds number on the longitudinal forces and moments were found to be nominal. However, the effects of Mach number and Reynolds number on the lateral-directional forces and moments were more pronounced. These effects only occurred at high angles of attack. Yawing moments became less nonlinear at the high Reynolds number test conditions. Compressibility was found to have a larger effect at high Reynolds numbers than was observed at low Reynolds numbers. In addition, the angle of attack at which Reynolds number effects became evident seems to have increased as Reynolds number itself increases.

Simple theoretical methods based upon linear theory were found to provide less accurate estimates of the longitudinal forces and moments than is usually achievd. This was due to the lack of representing the nonlinear wing-fuselage interaction effects as regards the leading edge vortex flow. Approximate estimates of the zero-lift drag coefficient were obtained at subcritical and supersonic conditions using conventional methodology.

References

1. Fox, C. H., Jr.; Luckring, J. M.; Morgan, H. L., Jr.; and Huffman, J. K. (1988): Subsonic Longitudinal and Lateral-Directional Static Aerodynamic Characteristics of a Slender Wing-Body Configuration. NASP TM-1011.
2. Fuller, D. E. (1981): Guide for Users of the National Transonic Facility. NASA TM 83124.
3. Jackson, C. M., Jr.; Corlett, W. A.; and Monta, W. J. (1981): Description and Calibration of the Langley Unitary Plan Wind Tunnel. NASA TP-1905.
4. McGhee, R. J.; Beasley, W. D.; and Foster, J. M. (1984): Recent Modifications and Calibration of the Langley Low-Turbulence Pressure Tunnel. NASA TP-2328.
5. Covell, P. F.; Wood, R. M.; Bauer, S. X. S.; and Walker, I. J. (1988): Experimental and Theoretical Evaluation of a Generic Wing Cone Hypersonic Configuration at Supersonic Speeds. Fourth National Aerospace Plane Symposium, Paper No. 83.
6. Luckring, J. M.; Fox, C. H., Jr.; and Cundiff, J. S. (1988): Reynolds Number Effects on the Subsonic Aerodynamics of a Generic Accelerator Configuration. Fourth National Aero-Space Plane Technology Symposium, Paper No. 82.
7. Keener, E. R.; and Chapman, G. T. (1974): Onset of Aerodynamic Sideforces at Zero Sideslip on Symmetric Forebodies at High Angles of Attack. AIAA Paper No. 74-770.
8. Margason, R. J.; and Lamar, J. E. (1971): Vortex-Lattice Fortran Program for Estimating Subsonic Aerodynamic Characteristics of Complex Planforms. NASA TN D-6142.
9. Lamar, J. E.; and Gloss, B. B. (1975): Subsonic Aerodynamic Characteristics of Interacting Lifting Surfaces with Sharp Edges Predicted by a Vortex-Lattice Method. NASA TN D-7921.
10. Polhamus, E. C. (1966): A Concept of the Vortex Lift of Sharp-Edged Delta Wings Based on a Leading-Edge-Suction Analogy. NASA TN D-3767.
11. Lamar, J. E.; and Luckring, J. M. (1979): Recent Theoretical Developments and Experimental Studies Pertinent to Vortex Flow Aerodynamics - With a View Towards Design. AGARD CP-247, Paper No. 24.
12. Luckring, J. M.; and Thomas, J. L. (1986): Separation Induced Vortex Flow Effects - Some Capabilities and Challenges. First National Aerospace Plane Technology Symposium.

13. Stahl, W.; Hartmann, K.; and Schneider, W. (1971): Kraft- und Druckverteilungsmessungen an einer Flugel-Rumpf-Kombination mit Flugel kleiner Streckung in kompressibler Stromung. DGLR / AVA-FB 7129.

14. Middleton, W. D.; Lundry, J. L.; and Coleman, R. G. (1980): A System for Aerodynamic Design and Analysis of Supersonic Aircraft. Part 1 - General Description and Theoretical Development. NASA CR-3351.

15. Sommer, S. C.; and Short, B. J. (1955): Free-Flight Measurements of Turbulent-Boundary-Layer Skin Friction in the Presence of Severe Aerodynamic Heating at Mach Numbers From 2.8 to 7.0. NACA TN 3391.

16. Compton, W. B., III (1972): Jet Effects on the Drag of Conical Afterbodies at Supersonic Speeds. NASA TN D-6789.

ORIGINAL PAGE IS
OF POOR QUALITY

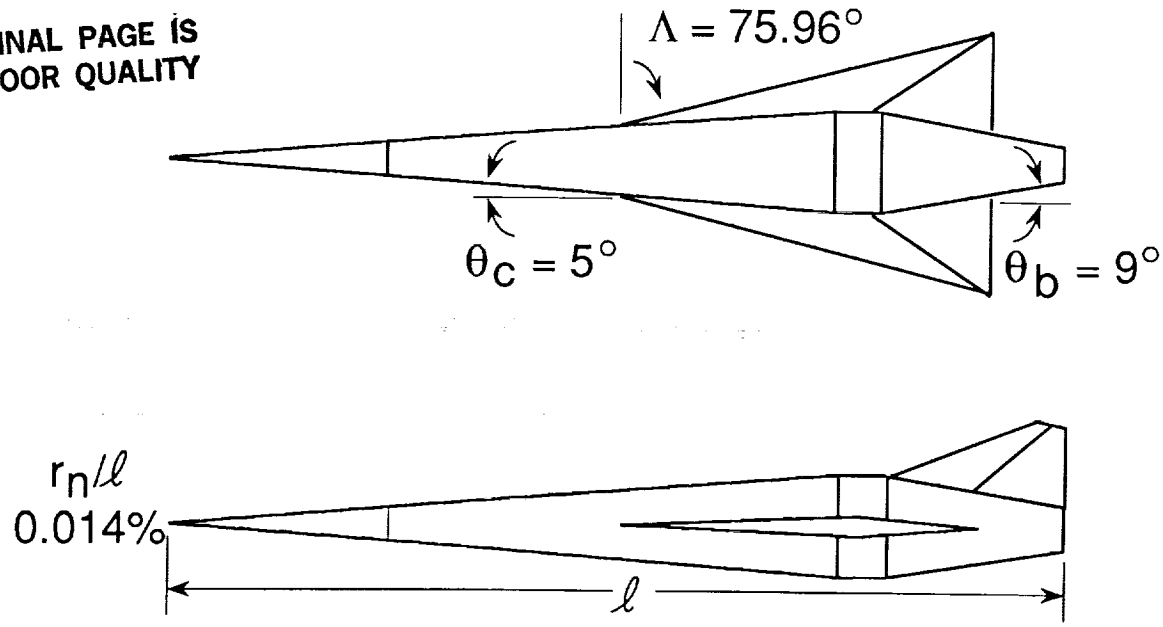

Figure 1.- Geometric features.

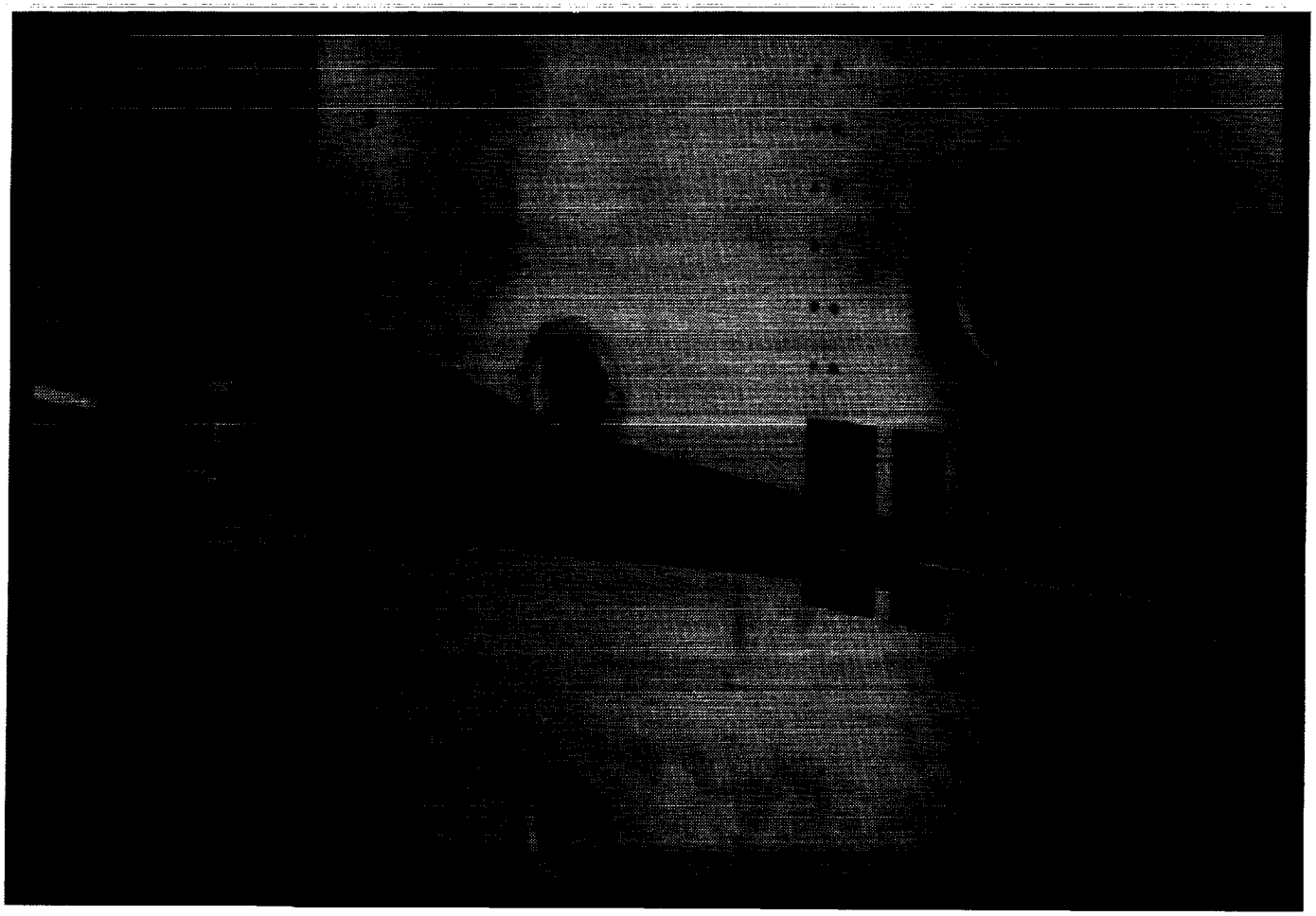

Figure 2.- Model mounted in NTF.

ORIGINAL PAGE
BLACK AND WHITE PHOTOGRAPH

ORIGINAL PAGE IS

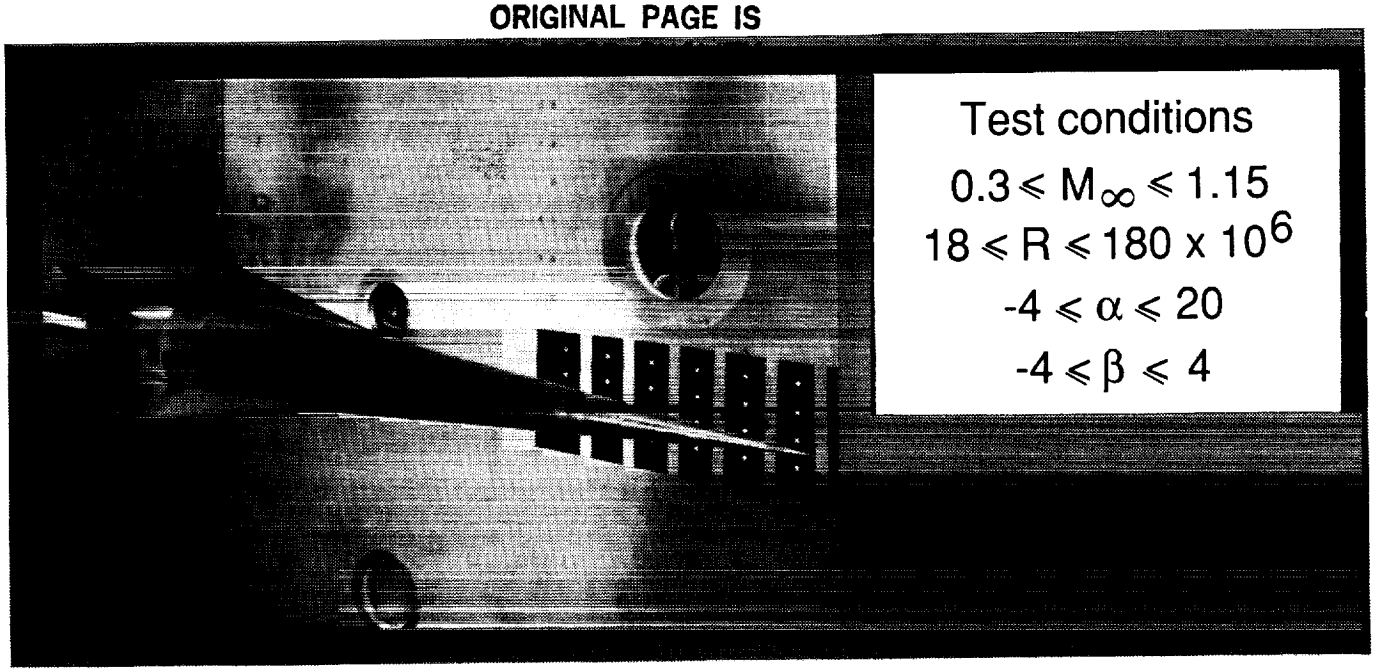

Figure 3.- Range of test conditions.

ORIGINAL PAGE
BLACK AND WHITE PHOTOGRAPH

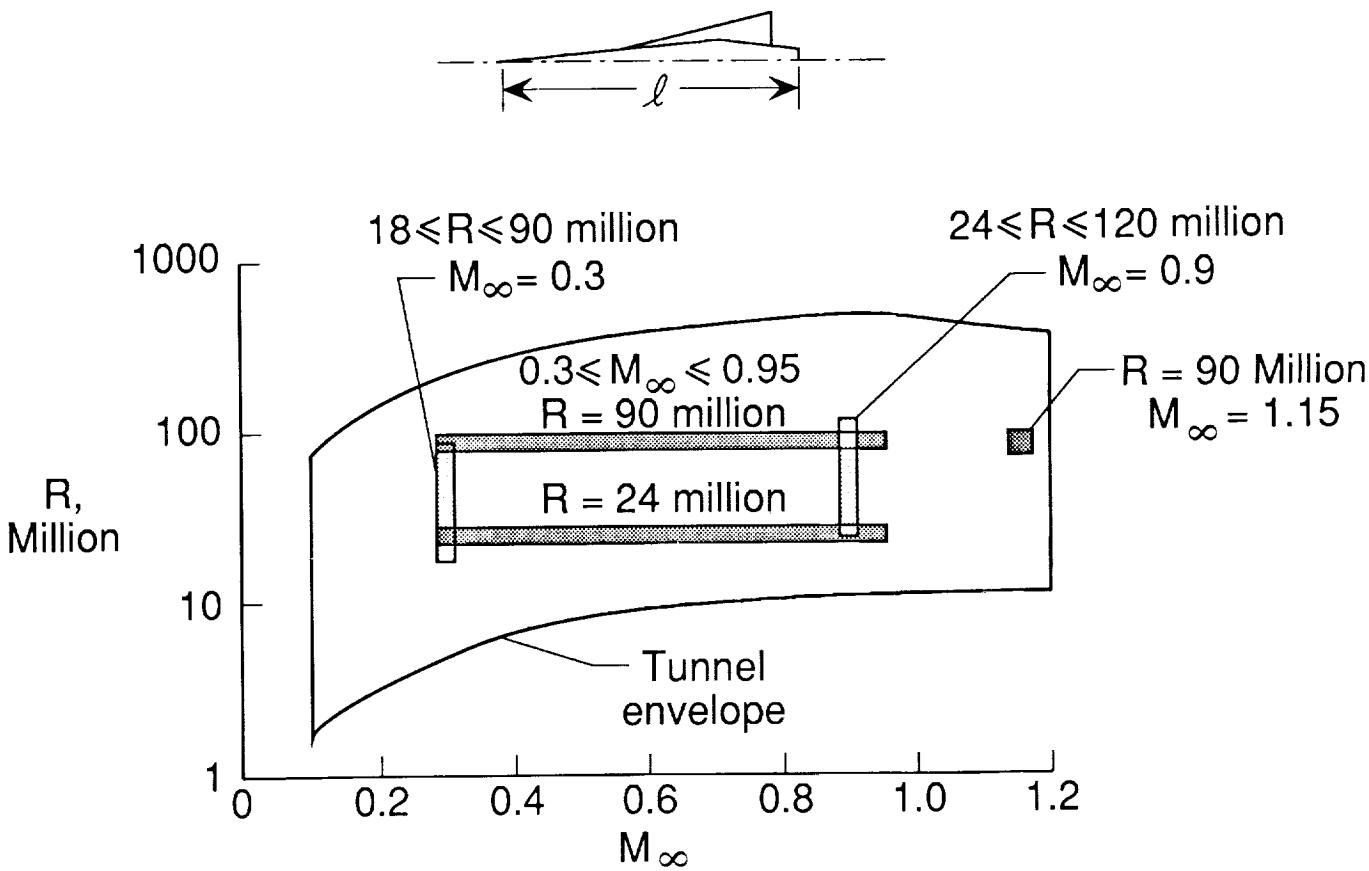

Figure 4.- Test program for NTF.

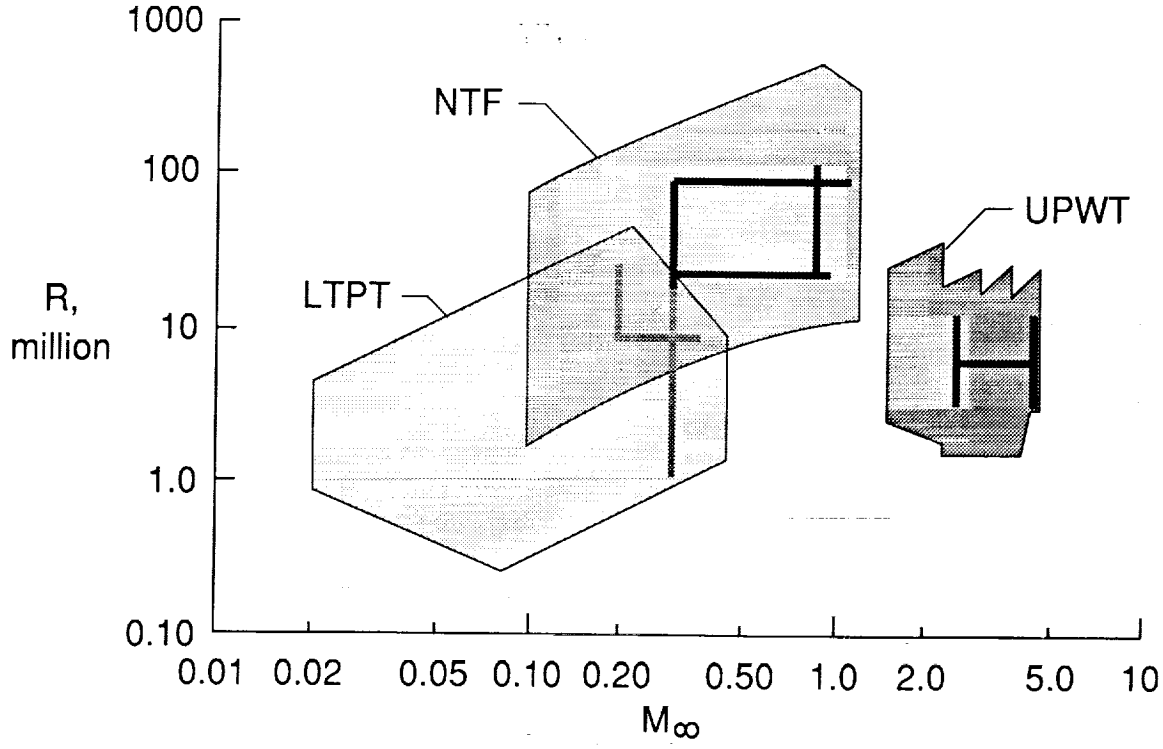

Figure 5.- Comprehensive test program.

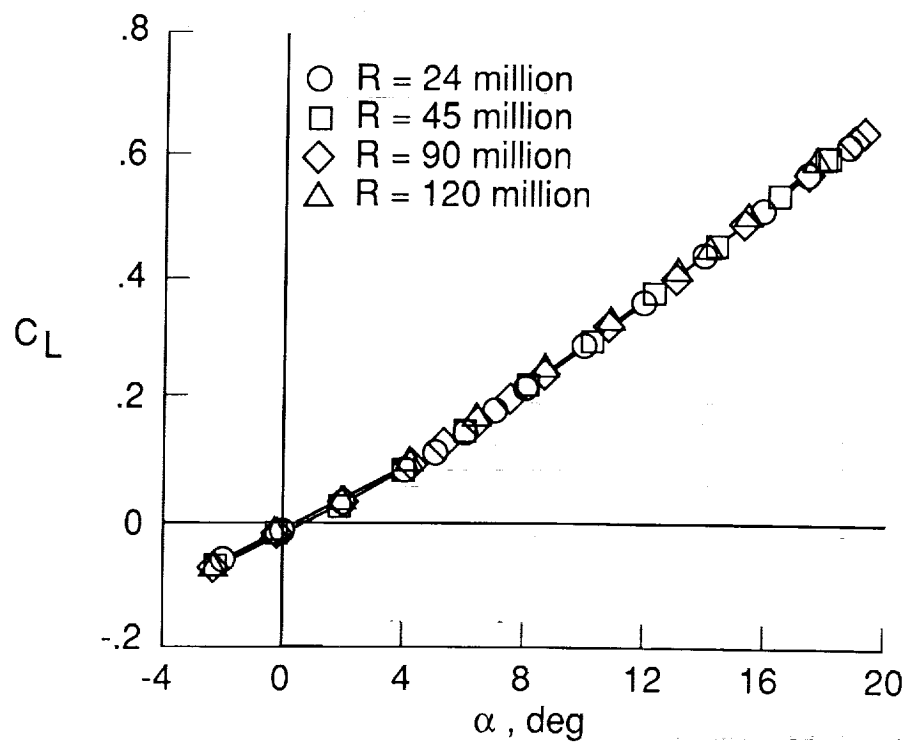

(a) Lift.

Figure 6.- Reynolds number effect on longitudinal aerodynamic properties. $M_\infty = 0.9$.

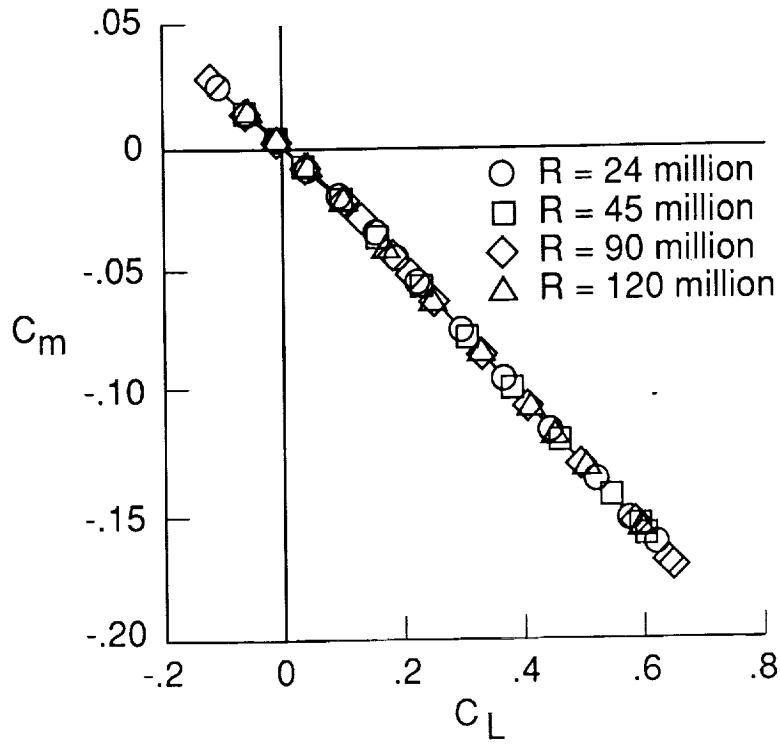

(b) Pitching moment.

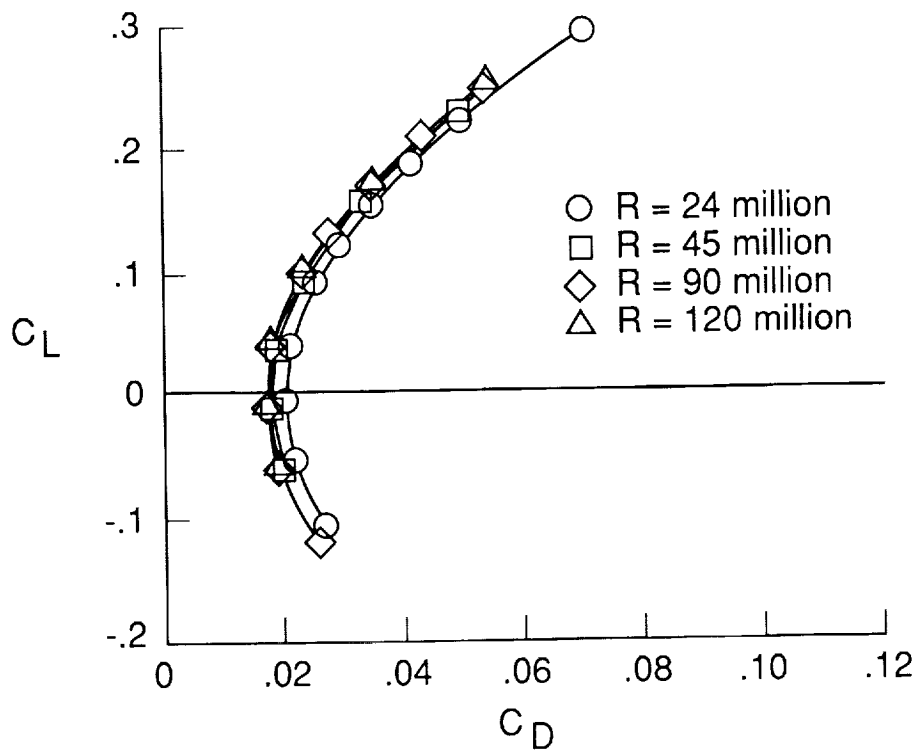

(c) Drag.

Figure 6.- Concluded.

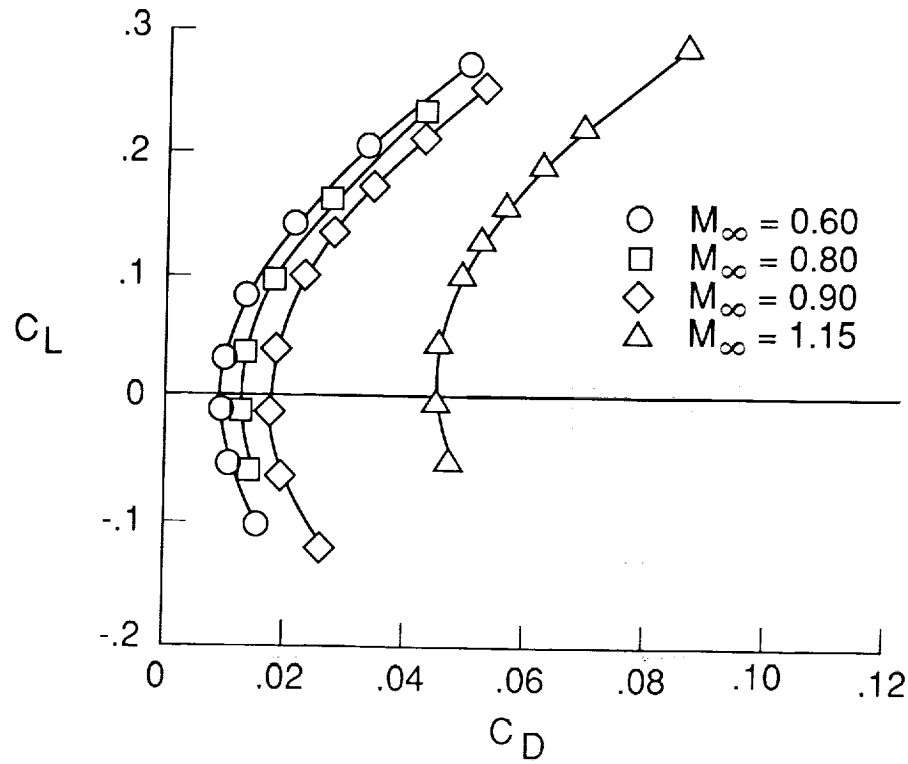

Figure 7.- Effect of Mach number on drag. R = 90 million.

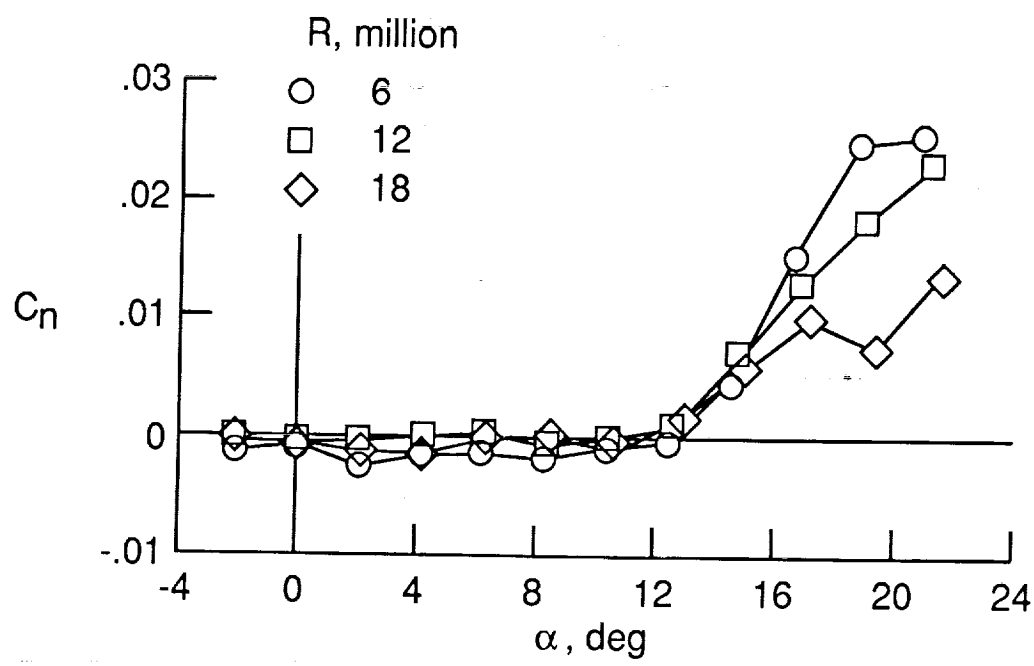

Figure 8.- Reynolds number effects on yawing moment. M_∞ = 0.3. After Luckring et al. (1988).

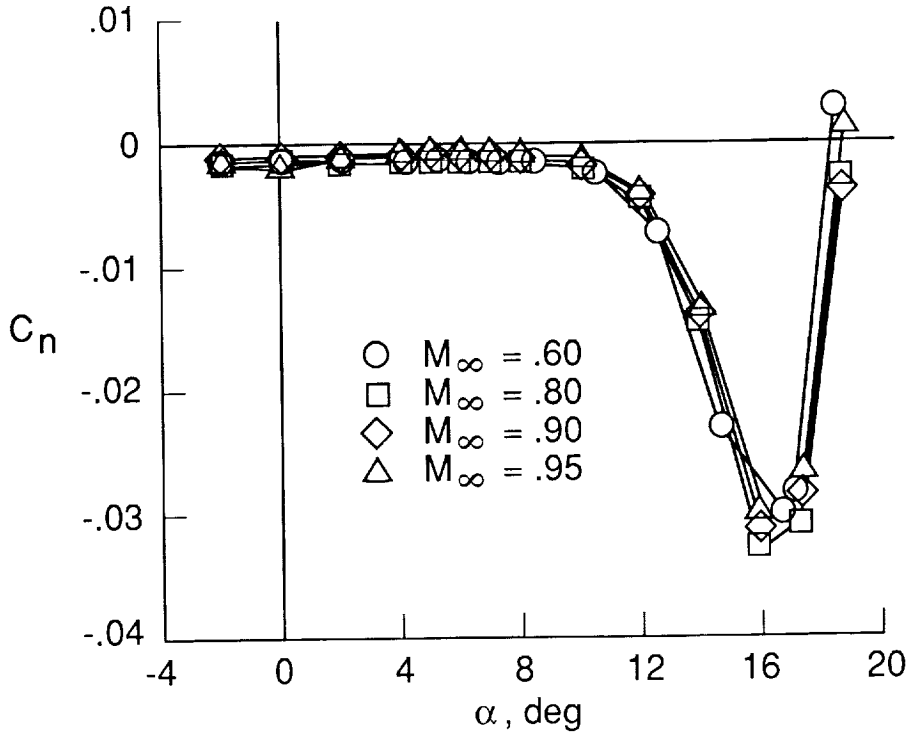

(a) R = 24 million.

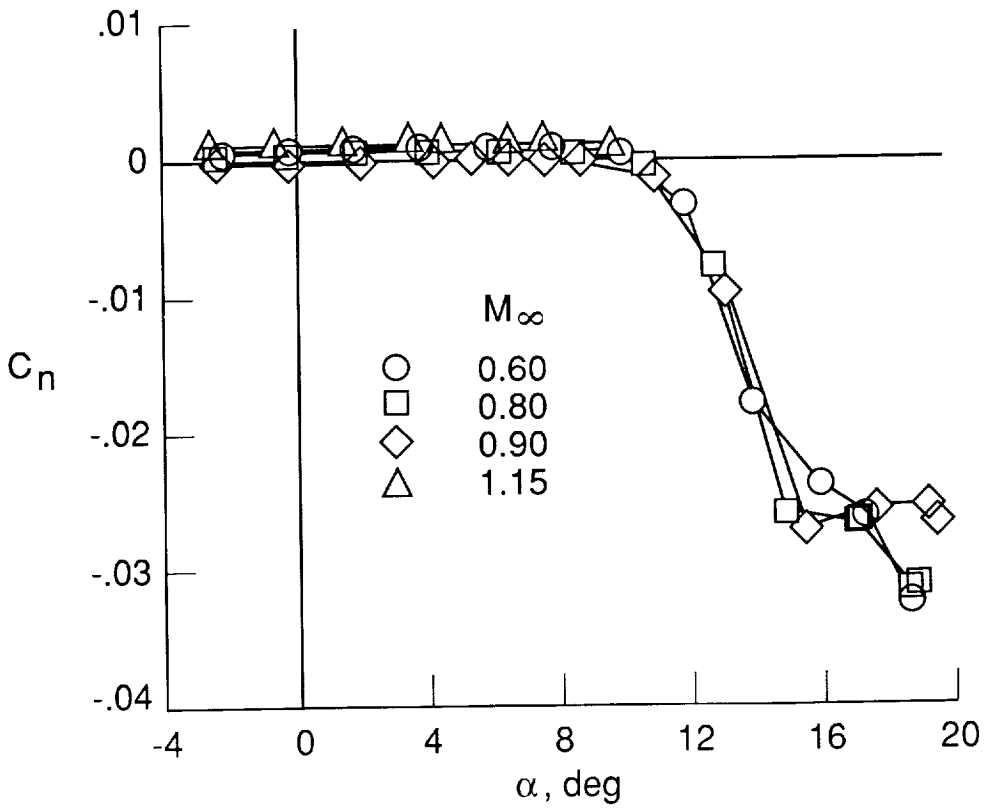

(b) R = 90 million.

Figure 9.- Effect of Mach number on yawing moment.

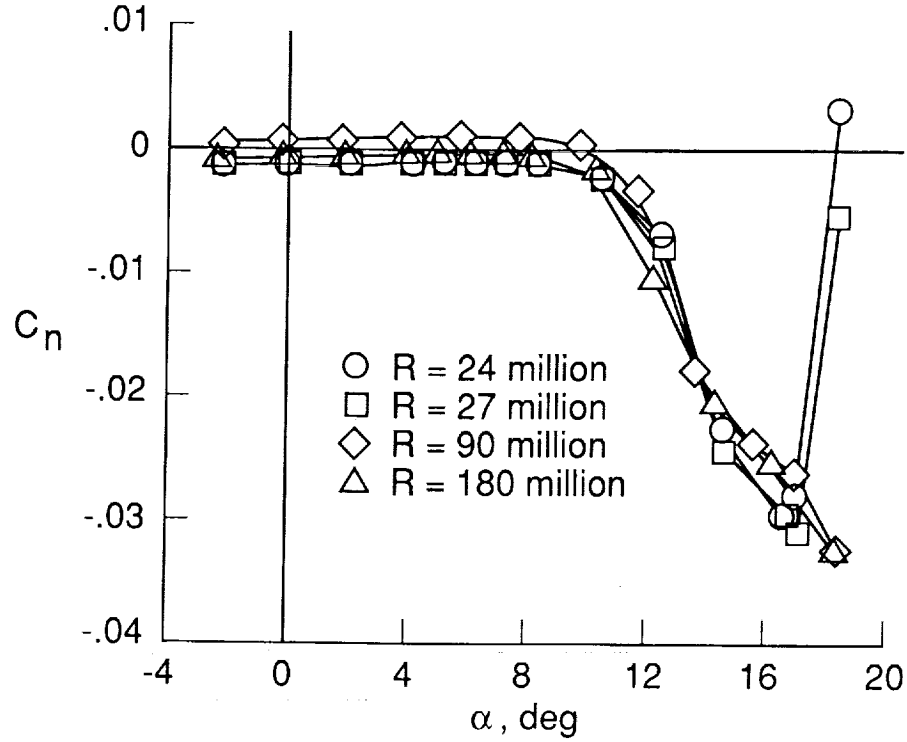

(a) $M_\infty = 0.6$

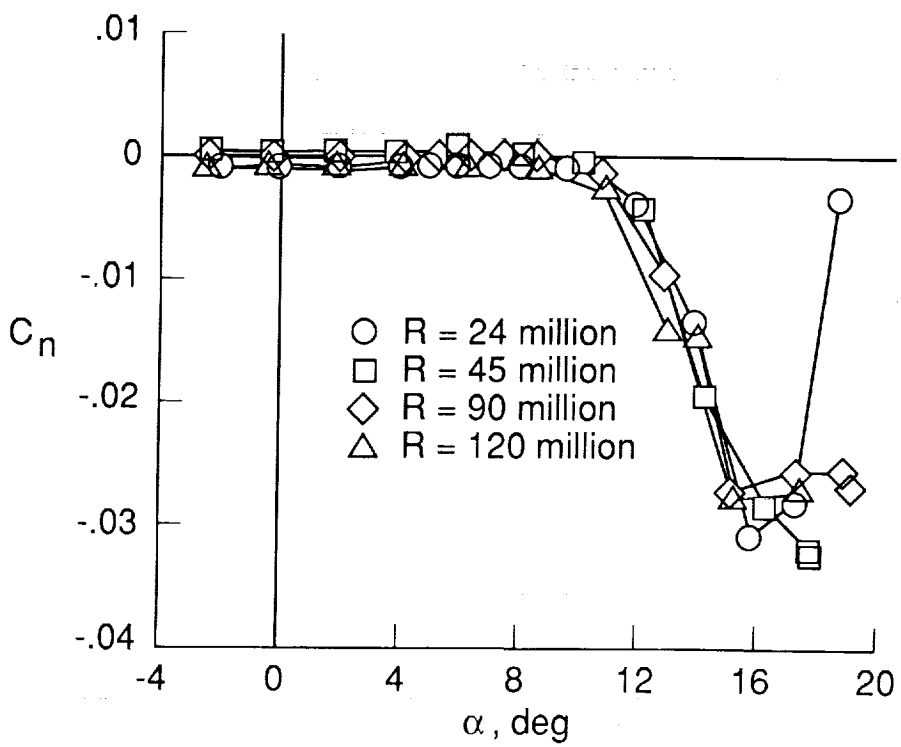

(b) $M_\infty = 0.9$

Figure 10.- Effect of Reynolds number on yawing moment.

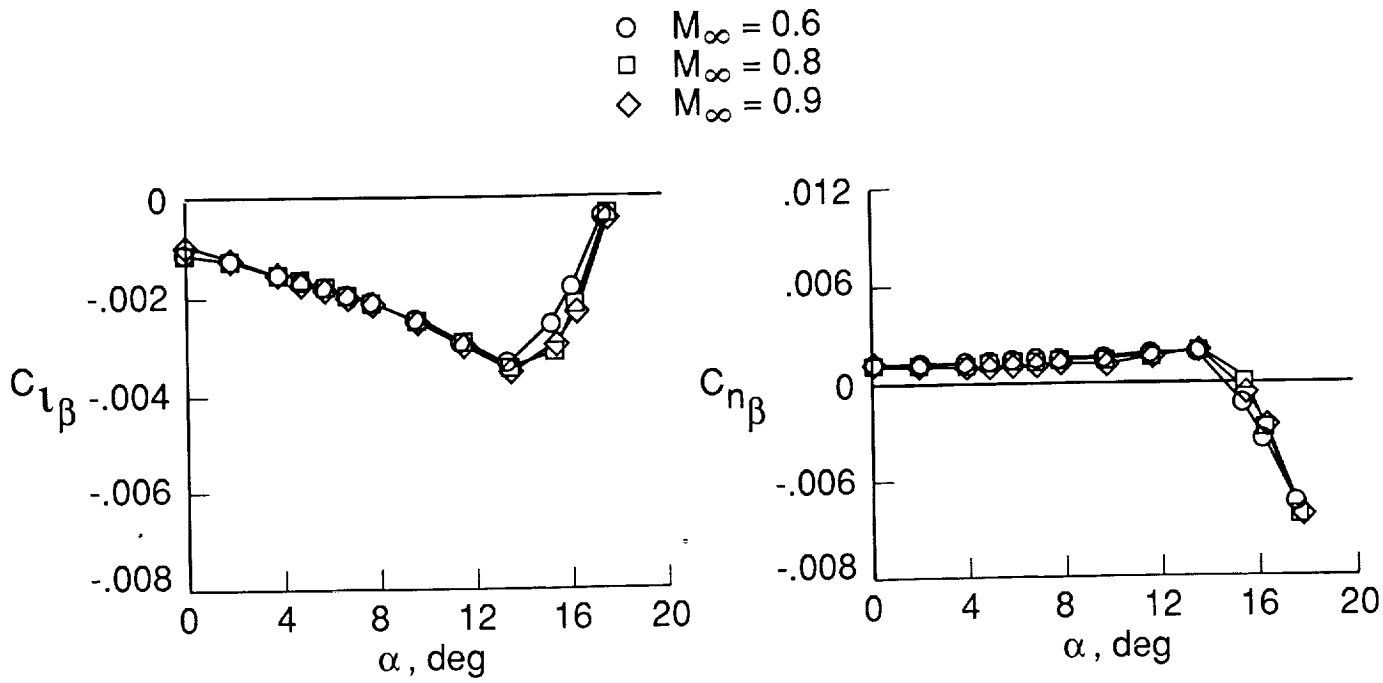

(a) R = 24 million.

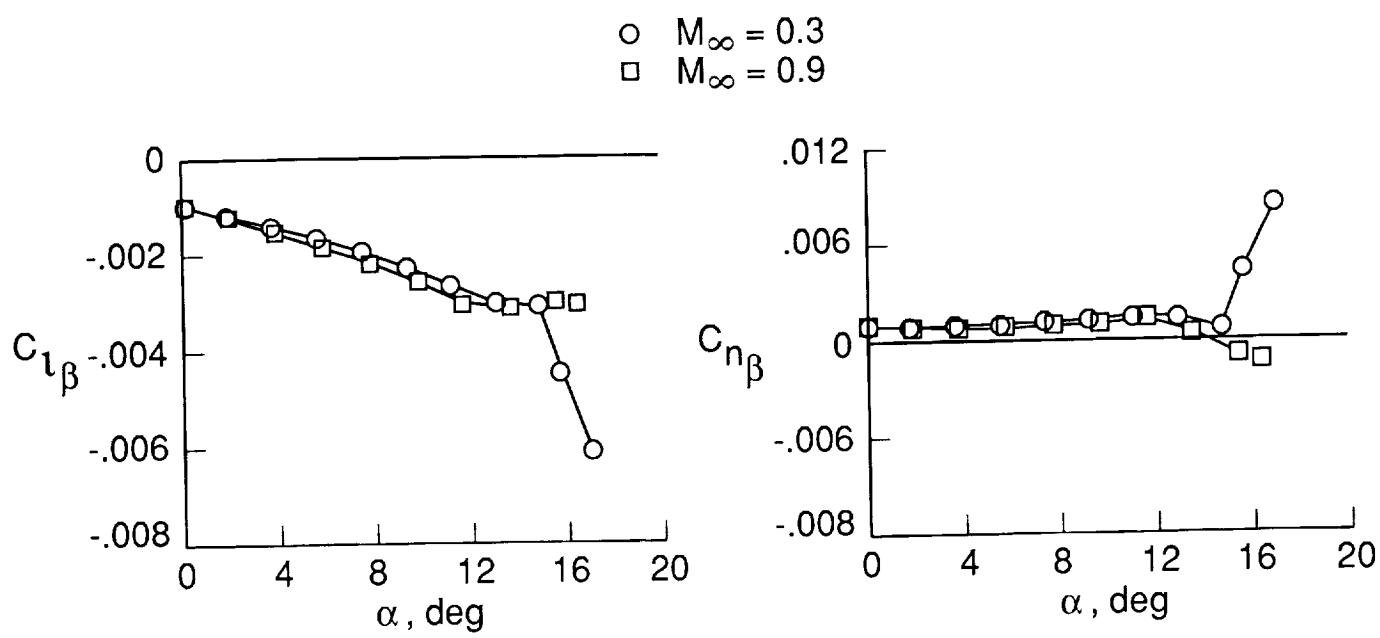

(b) R = 90 million.

Figure 11.- Effect of Mach number on lateral-directional stability.

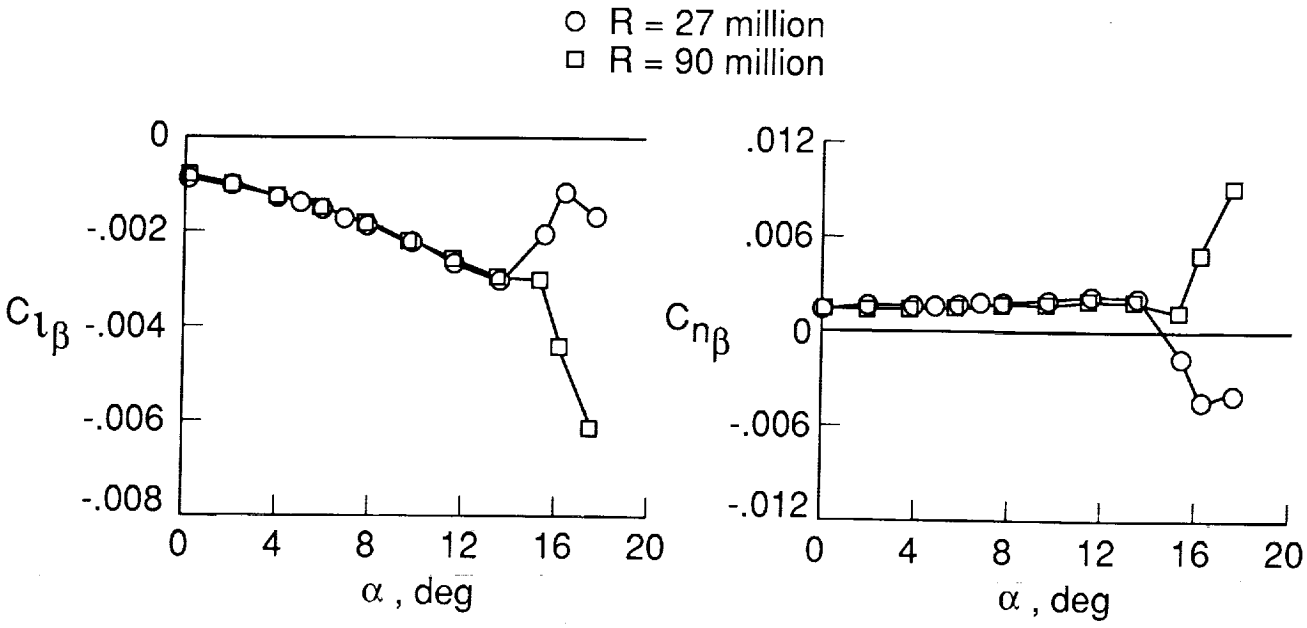

(a) $M_\infty = 0.3$

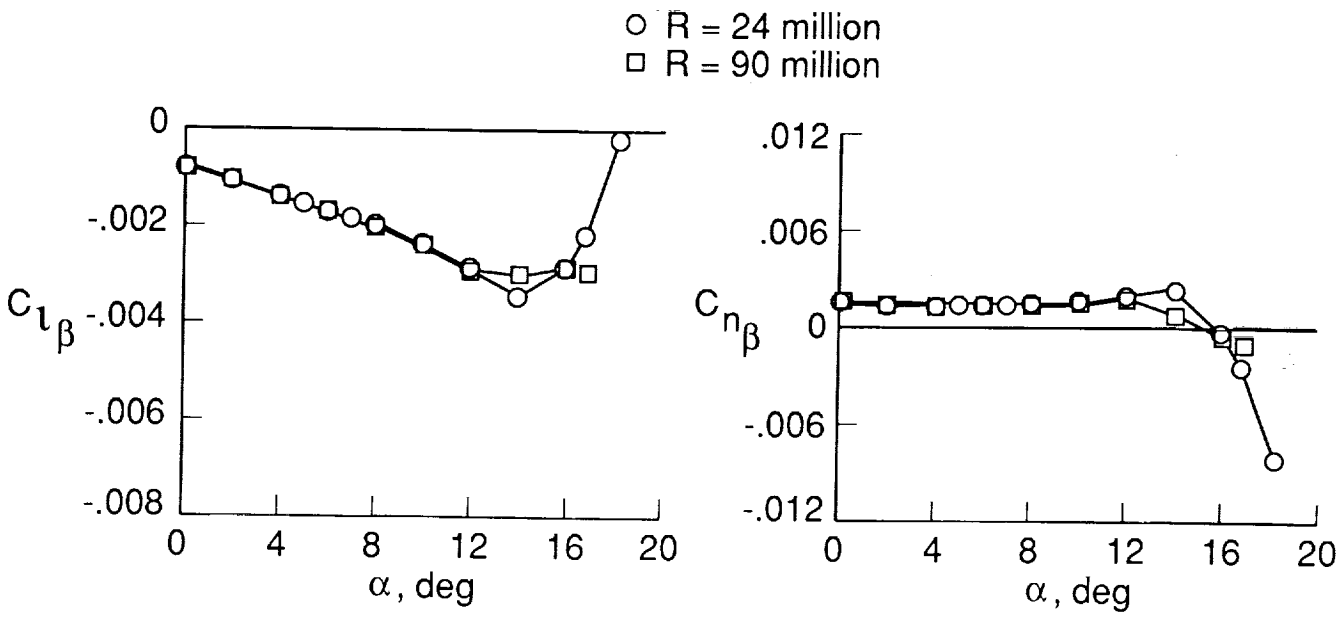

(b) $M_\infty = 0.9$

Figure 12.- Effect of Reynolds number on lateral-directional stability.